Quantum MCMC algorithm for spin glass ground state search: an application to parameter calibration

Maria Popovic, G2Q Computing

1 Industrial use-case: longitudinal dynamics of a drone

The longitudinal dynamics of a small quadrotor is described by the equation

$$a_x(t) = X_u(t)u(t) + X_q(t)q(t) + X_\delta(t)\delta_{lon}(t), \tag{1.1}$$

derived from Newton-Euler's equation. Here, $a_x(t)$ is the drone's longitudinal acceleration, $u(t)$ is its velocity component along the x axis, $q(t)$ is the pitch rate, $\delta_{lon}(t)$ the normalised pitch moment.

In this model, $u(t)$, $q(t)$, $\delta_{lon}(t)$ and $a_x(t)$ are determined through a set of experimental measurements.

The parameters X_u and X_q are stability derivatives, while X_δ is a control derivative [1]. These quantities can be in general time dependent. For a set of values $\left(X_u, X_q, X_\delta\right)$, the longitudinal acceleration $a(t)$ is calculated from Eq. (1.1). For the data provided, $X_\delta^{sol} = -3.96101\ m\ s^{-2}$.

The stability derivatives for this particular experiment are known to be

$$X_u^{sol} := -0.93260\ s^{-1}, \tag{1.2}$$

$$X_q^{sol} := -0.64995\ m\ s^{-1}, \tag{1.3}$$

and will provide benchmark values for the algorithm described in this work.

The aim of this work is to build a quantum hybrid algorithm that is able to find the values in Eq. (1.2).

2 Encoding into an Ising model Hamiltonian

The possible values of the two stability derivatives are indicated as X_u, X_q. The MCMC algorithm searches a space of states for the optimal solution. Each state encodes a couple of possible values $|X_u, X_q\rangle$.

The question we want to answer is how to define a Hamiltonian whose eigenstates are the states $|X_u, X_q\rangle$, encoding the possible values of the parameters X_u, X_q during the random walk, and whose eigenvalues are the cost functions associated to those parameter values. $\hat{H}_{cost}$ should, in short, satisfy the equation

$$\hat{H}_{cost}|X_u, X_q\rangle = \frac{1}{N}\sum_x \left(a_x(X_u, X_q) - a_x^{data}\right)^2 |X_u, X_q\rangle, \tag{2.1}$$

where N is the number of x samples. In the case of Eq. (2.1), we chose the cost function to be the mean squared error with respect to a data set a_x^{data}, but it can in general be a cost function of choice. In the model considered here, a_x is the longitudinal acceleration function.

The aim is to translate the mean squared error into a spin glass system described by an Ising model. The ground state of this spin glass system is the state that minimizes the mean squared error with respect to the data, and thus is the solution to the problem.

A complex calculation with quantum operators leads to the result

$$\begin{aligned}\hat{H}_{cost} = &-\sum_{s=0}^{r-1}\sum_{j=0}^{r-1}\sum_{t=0}^{r-1}\sum_{k=0}^{r-1} J_{sjtk}\hat{Z}_s^0\hat{Z}_j^0\hat{Z}_t^1\hat{Z}_k^1 - \sum_{\alpha=0,1}\sum_{s=0}^{r-1}\sum_{j=0}^{r-1}\sum_{k=0}^{r-1} J_{sjk}^\alpha\hat{Z}_s^0\hat{Z}_j^\alpha\hat{Z}_k^1 \\ &- \sum_{\alpha=0,1}\sum_{j>k=0}^{r-1} J_{jk}^\alpha\hat{Z}_j^\alpha\hat{Z}_k^\alpha - \sum_{j=0}^{r-1}\sum_{k=0}^{r-1} J_{jk}^{01}\hat{Z}_j^0\hat{Z}_k^1 - \sum_{\alpha=0,1}\sum_{j=0}^{r-1} h_j^\alpha\hat{Z}_j^\alpha + L\hat{\mathbb{I}}_{2r}.\end{aligned} \tag{2.2}$$

where $\hat{Z}_j^\alpha$ is the Pauli operator along the z axis acting on the spin in position j in the subspace α. $\alpha = 0, 1$ with "0" being the subspace associated with X_u, and "1" the subspace associated with X_q, such that $|X_u, X_q\rangle = |X_u\rangle_0|X_q\rangle_1$.

The coupling strength parameters J and magnetic fields h are engineered from the data. Here r is the number of spins for each subspace α, for a total of $2r$ spins.

The time evolution operator that we are going to apply to the two-parameter state $|X_u\rangle_0|X_q\rangle_1$ is

$$\hat{H} = (1-\gamma)\alpha_n \hat{H}_{cost} + \gamma \hat{H}_{mix}, \tag{2.3}$$

with $\hat{H}_{cost}$ defined by Eq. (2.2). $\hat{H}_{mix}$ is a mixing Hamiltonian defined as

$$\hat{H}_{mix} = \sum_{\alpha=0,1} \sum_{j=0}^{r-1} \hat{X}_j^{\alpha}, \tag{2.4}$$

and α_n, γ are set by heuristic methods.

We divide the four-body, three-body, two-body and one-body interaction terms by re-defining the elements of Eq. (2.2) and $\hat{H}_{mix}$ as $\hat{H}_4$, $\hat{H}_3$, $\hat{H}_2$ and $\hat{H}_1$ respectively. We can write a second-order Trotter splitting formula for the time-evolution operator, leading to

$$\hat{\tilde{V}} = e^{-i\Delta t \hat{H}_1} \left(e^{-i\Delta t \hat{H}_2} e^{-i\Delta t \hat{H}_3} e^{-i\Delta t \hat{H}_4} e^{-i\Delta t \hat{H}_1} \right)^{b-1}. \tag{2.5}$$

Here the total evolution time t has been divided into b slices, $t = b\Delta t$.

3 Developing the algorithm

The goal is to use a Metropolis-Hastings algorithm to find the ground state of the spin glass problem Hamiltonian $\hat{H}_{cost}$.

How to build an algorithm that can find a low energy state with better than random-guessing probability?

A generic way to guarantee that at each MCMC step, the energy expectation of Hamiltonian $\hat{H}_{cost}$ is lowered by the quantum random walk, is to start each step iteration in the ground state of the walk Hamiltonian $\hat{H}_{mix}$ [2]. This comes as a consequence from the conservation of energy. Indeed, for any final time t_f,

$$\frac{1}{t_f} \int_{t=0}^{t_f} \langle \hat{H}_{cost} \rangle_{\psi(t)} dt < \langle \hat{H}_{cost} \rangle_{\psi(0)}. \tag{3.1}$$

Starting from a ground state of $\hat{H}_{mix}$ guarantees that the time evolution lowers the energy expectation value of $\hat{H}_{cost}$. A measurement in the computational basis thus gives an output state with lower energy than the input state.

The *quantum Metropolis - Hastings algorithm* is proposed as follows:

1. To initialize the algorithm, a state $(X_u^{(0)}, X_q^{(0)})$ is extracted with uniform probability from the set of possible 2^{2r} states. The value of the cost function (energy of the cost Hamiltonian $\hat{H}_{cost}$) corresponding to the extracted state is computed and stored classically.

2. At step $j = 0$, state $|-\rangle^{\otimes 2r}$ is set as the input state in the quantum circuit. The initial distribution is thus uniform. Note that $|-\rangle^{\otimes 2r}$ is the ground state of the mixing Hamiltonian $\hat{H}_{mix} = \sum_{\alpha} \sum_{j=0}^{r-1} \hat{X}_j^{\alpha}$.

3. State $|-\rangle^{\otimes 2r}$ is evolved in the quantum circuit for a time $T = b\Delta t$, where b is suitably chosen. A measurement is performed at T, with output state $|\psi(T)\rangle_{j=0}$. The probability amplitudes of the canonical basis stases in state $|\psi(T)\rangle_{j=0}$ are retrieved.

4. The number of canonical basis states measured in the output state $|\psi(T)\rangle_{j=0}$ is $N_1 \leq 2^{2r}$. To further reduce the dimension of the searched state space, a selection is made on the output basis states, based on the respective probability of measurement. Basis states measured with a probability p such that $p \geq C/N_1$ are selected, where $0 < C < N_1$ is an arbitrarily chosen number. This selects a number $\bar{N}_1 < N_1$ of basis states.

5. A single couple of values $(X_u^{(1)}, X_q^{(1)})$) is classically extracted from a uniform distribution of the $\bar{N}_1$ selected states.

6. The value of the cost function (energy of the cost Hamiltonian) corresponding to the extracted state is computed and stored.

7. The energy of the new state $(X_u^{(1)}, X_q^{(1)})$ is classically compared to the energy of the previous state $(X_u^{(0)}, X_q^{(0)})$, and $(X_u^{(1)}, X_q^{(1)})$ is either accepted and stored in place of $(X_u^{(0)}, X_q^{(0)})$, or rejected and discarded, according to the accept-reject MH function.

8. The circuit is again initialized in state $|-\rangle^{\otimes 2r}$ with $\hat{H}_{mix} = \sum_\alpha \sum_{j=0}^{r-1} \hat{X}_j^\alpha$ and evolved for a time $T = b\Delta t$.

9. The procedure described in points [2.] – [6.] is repeated for a number j_{max} of steps.

The quantum Metropolis - Hastings algorithm is guaranteed to find a lower energy state for $\hat{H}_{cost}$ at each step with respect to the cost energy associated with state $|-\rangle^{\otimes 2r}$. However, it does not guarantee that the state measured at step j is at a lower cost energy with respect to the state accepted at step $j-1$. In fact, in this procedure one always selects a number $\bar{N}_j$ of states from the same distribution, because the measured state $|\psi(T)\rangle_j$ is always the same at fixed T, $\forall j$.

The quantum advantage might then arise from simply reducing the searched state space, first by performing a measurement at a suitable time, then by classically discarding states based on their probability of measurement.

The quantum MH algorithm is compared to a classical MH algorithm where the dynamics is defined by a stochastic matrix $P(t)$ generated by the Laplacian L,

$$P(t) = e^{-tL}, \ \forall t \geq 0, \tag{3.2}$$

where the Laplacian is related to the quantum Hamiltonian through $L_{jk} = -|(\hat{H}_{mix})_{jk}|^2$, $L_{jj} = \sum_{s\neq j} |(\hat{H}_{mix})_{js}|^2$ [3].

4 Testing the algorithm

The integer value $b \geq 1$ is the number of times the Trotterized time evolution gate is applied in a single call to the quantum circuit. At each step of the MCMC, the measurement time is then $T = b\Delta t$. What is the optimal time T at which to perform a measurement on the circuit, so that the probability of measuring the ground state is highest? Figs. 1show the circuit outputs. In particular, they show there exists a measurement time for which

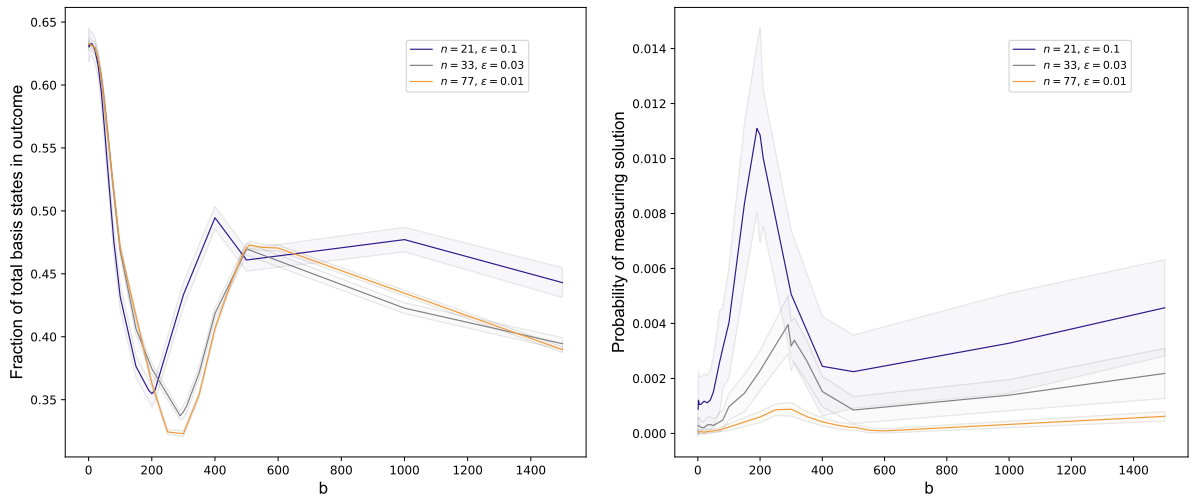


Figure 1: Left: Fraction of canonical basis states measured in output over the possible $D_r = 2^{2r}$ states of the Hilbert space, for the two-variable (X_u, X_q) calibration circuit, as a function of the number of time-steps b after which the measure is performed. Right: Probability of measuring the solution state $|X_u^{sol}\rangle|X_q^{sol}\rangle$ in output, as a function of the number of time-steps b. For both figures, the plot is shown for three different encoding quantization levels $n = 21, 33, 77$ corresponding to a number $2r = 10, 12, 14$ of spins respectively. The reached precision ϵ from the true solution is also shown in the legend. The solid lines show the average over 50 runs of the circuit, with the bands representing the standard deviation. Each measurement is taken over 2^{2r} shots. The input state is $|-\rangle^{\otimes 2r}$.

the output fraction of canonical basis states over the existing $D_r = 2^{2r}$ states is lowest. This corresponds to a higher probability of measuring the solution state. This is not surprising, as the fewer the canonical basis states with non-zero probability amplitude, the larger the amplitudes will be. Figs. 1 also show that the probability of measuring the solution state is never zero.

The minimum location in Fig. 1, left, is at $b \approx 200, 290, 300$ for $n = 21, 33, 77$ respectively.

5 Comparison of performance between classical and quantum hybrid algorithm

The quantum MH algorithm discussed in this work is able to gain a significative speedup in finding the ground state of a complex system with respect to its classical counterpart. This speedup is due to the quantum walk's ability to reduce the total searched state space to a subspace of relevant low-energy states, if a measurement on the system is performed at an appropriate time. The quantum system is designed such that its energy eigenvalues E_{cost} equal the classical mean squared error function with respect to the data. The algorithm naturally converges to smaller and smaller values of the mean squared error, eventually finding the ground state. The ground state is the state representing the values of the parameters that best fit the given data, as much as the reachable precision allows, out of all possible states. The reachable precision is set by the number of spins in the system, or equivalently, by the number of qubits in the quantum circuit.

The quantum circuit that simulates the time evolution of the system is gate based, and is designed to run on gate based quantum hardware, such as IBM quantum machines.

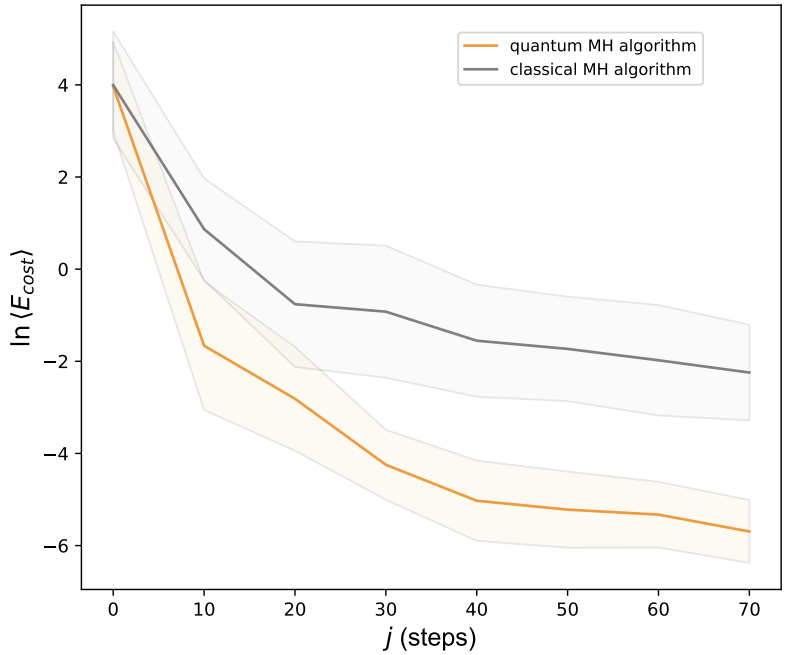


Figure 2: Logarithm of the average value of the cost energy (eigenvalue of the Hamiltonian $\hat{H}_{cost}$ for the quantum algorithm, mean squared error for the classical algorithm) measured at step j, as a function of the total number of steps in the MCMC algorithm. The figure compares the results of the classical MH algorithm (grey line) with that of the quantum MH algorithm (orange line). Here the most complex case for two parameters (X_u, X_q) is considered, where the quantization level of the variables' interval is $n = 77$. Both classical and quantum algorithm search a state space with high dimension $D_r = 2^{14}$. The average is taken over 20 runs for the quantum MH, 40 runs for the classical MH. The error bands represent the respective standard deviations of the simulations. The annealing schedule for the Metropolis - Hastings MCMC algorithm $\beta(j)$ is taken to be exponential with coefficient $k = 0.3$.

The rate at which the average value of the mean squared error E_{cost} decreases, as the Metropolis - Hastings MCMC walks more steps, is shown in Fig. 2 for both the quantum algorithm and its corresponding classical algorithm. The figure shows that for any given number of steps j the quantum algorithm outputs values of $\left(X_u, X_q\right)$ such that the drone's acceleration calculated with these parameters fits the real data better than the classical output. Overall, the quantum algorithm is converging faster than the classical one to the lowest energy value possible. For example, for the last point in the figure, at $j = 70$ steps, the average cost energy reached by the quantum algorithm is $\langle E_{cost}\rangle = 0.003$, while for the classical it is $\langle E_{cost}\rangle = 0.106$.

A widely used figure of merit for evaluating the speed of an MCMC algorithm in finding the ground state of a

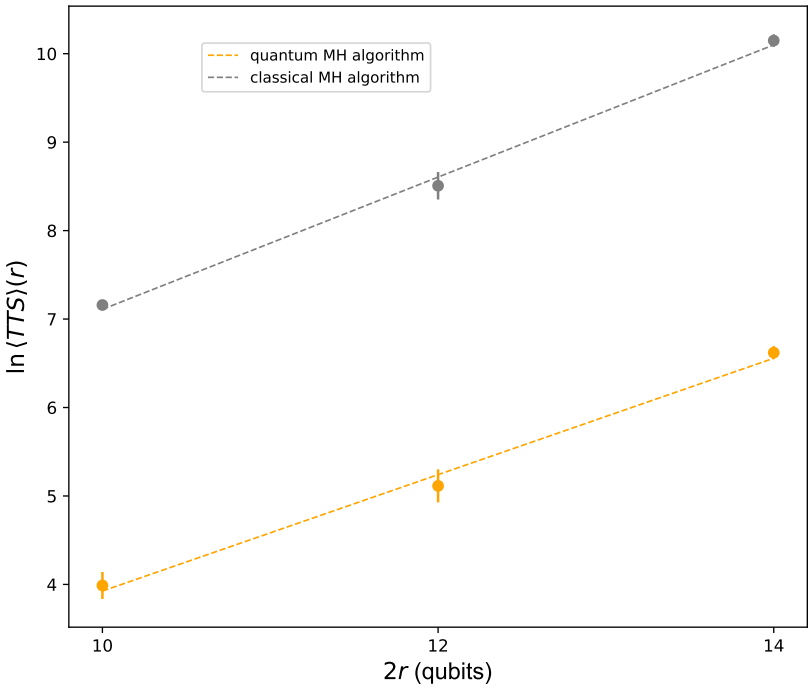


Figure 3: Logarithm of the average value of the TTS as a function of the number of qubits $2r$ for the calibration of the two parameters (X_u, X_q). The grey points represent the classical MH algorithm's results, the orange points represent the results of the quantum algorithm. Grey and orange dashed lines are the linear curve fits of the respective points. Each point represents the number of steps necessary to reach the solution with target probability $\delta = 90\%$, within precision $\epsilon = 0.1, 0.03, 0.01$ for a number of qubits $2r = 10, 12, 14$ respectively. The average is taken over 10 runs for the quantum MH, 5 runs for the classical MH. The error bars represent the respective standard deviations of the simulations. The annealing schedule for the Metropolis - Hastings MCMC algorithm $\beta(j)$ is taken to be exponential with coefficient $k = 0.3$.

system, is the time to solution (TTS). The time to solution is an estimate of the minimum number of steps necessary for the algorithm to find the ground state with a chosen success probability; in our case, $\delta = 90\%$. The ground state corresponds to the optimal solution allowed by the reachable precision; because in the case considered, the actual values of X_u and X_q are known, it is expected that both quantum and classical algorithm will reach the known solution within a fixed precision. Note that the precision is different from the resolution: the resolution indicates the number of decimal points with which the algorithm is computing the values of the parameters $\left(X_u, X_q\right)$. The precision ϵ, on the other hand, is only used in the computation of the TTS for comparison with a known solution. Precision and resolution are of course related, the resolution having to be $\leq \epsilon$.

In Fig. 3 the TTS is shown as a function of the number of qubits (spins) $N = 2r$. Indeed, the points shown are the average number of steps after which the algorithm will keep finding the state $\left(X_u, X_q\right) = (-1.0, -0.5)$ with probability $\geq 90\%$ in the case of $N = 10$ qubits, the state $\left(X_u, X_q\right) = (-0.94, -0.62)$ with probability $\geq 90\%$ in the case of $N = 12$ qubits and the state $\left(X_u, X_q\right) = (-0.92, -0.66)$ with probability $\geq 90\%$ in the case of $N = 14$ qubits. The known true solution for the model is $\left(X_u, X_q\right) = (-0.9, -0.6)$ rounded to one decimal point, and

Spins	MH algorithms result	True value	Classical TTS	Quantum TTS
$N = 10$	$\left(X_u, X_q\right) = (-1.0, -0.5)$	$\left(X_u, X_q\right) = (-0.9, -0.6)$	1286 ± 18	55 ± 2
$N = 12$	$\left(X_u, X_q\right) = (-0.94, -0.62)$	$\left(X_u, X_q\right) = (-0.93, -0.65)$	5000 ± 326	169 ± 10
$N = 14$	$\left(X_u, X_q\right) = (-0.92, -0.66)$	$\left(X_u, X_q\right) = (-0.93, -0.65)$	25600 ± 797	752 ± 17

Table 1: Ground state values found by the classical and quantum MH algorithms compared to the true values of the parameters, for varying number of spins, allowing for finer resolution.

$\left(X_u, X_q\right) = (-0.93, -0.65)$ rounded to two decimal points. Thus, the solutions found by both the algorithms in all three cases coincide with the known solution for the model. Tab 1 illustrates these results.

Fig. 3 shows that the quantum algorithm greatly outperforms the corresponding classical algorithm in terms of the time necessary to reach the ground state (equivalently, the solution to the problem). For a Hilbert space of dimension $D_r = 2^{10}$, the classical MH algorithm has $TTS = 1286$ against $TTS = 55$ for the quantum algorithm. For $D_r = 2^{12}$, the classical algorithm has $TTS = 5000$, the quantum algorithm $TTS = 169$. For $D_r = 2^{14}$, the classical algorithm has $TTS = 25600$, the quantum algorithm $TTS = 752$. Note that searching for a single state in a space of 2^{14} states is a complex problem for the classical MH algorithm, and the dimension is too high for any kind of matrix computation; it is however a manageable problem for the quantum MH algorithm. The dashed lines in Fig. 3 represent linear curve fits of the computed points, which are

$$\ln\langle TTS\rangle = 0.6561N - 2.623 \tag{5.1}$$

for the quantum MH algorithm, and

$$\ln\langle TTS\rangle = 0.7478N - 0.3642 \tag{5.2}$$

for the classical MH algorithm. This mean that the average quantum TTS, $\langle TTS\rangle_q$, is

$$\langle TTS\rangle_q \cong 0.1\langle TTS\rangle_c^{0.8774}, \tag{5.3}$$

with $\langle TTS\rangle_c$ the average classical TTS.

Thus, while the TTS of the quantum MH algorithm designed in this work still scales exponentially with the size of the system, $O(e^{0.6561N})$, the less-than-one exponent indicates a quantum advantage. The quantum advantage becomes more significant as the complexity of the problem increases.

References

[1] Ingabire, A. and Sklyarov, A. A., E3S Web Conf. **104**, 02001 (2019).

[2] A. Callison, N. Chancellor, F. Mintert, and V. Kendon, New Journal of Physics **21**, 123022 (2019).

[3] M. Frigerio, C. Benedetti, S. Olivares, and M. G. A. Paris, Phys. Rev. A **104**, L030201 (2021).